Chem. Mater. **2004,** *16,* 1597−1602

Stoichiometric Synthesis of Pure MFe_2O_4 (M = Mg, Co, and Ni) Spinel Ferrites from Tailored Layered Double Hydroxide (Hydrotalcite-Like) Precursors

Feng Li,* Junjie Liu, David G. Evans, and Xue Duan*

Education Ministry Key Laboratory of Science and Technology of Controllable Chemical Reactions, P.O.Box 98, Beijing University of Chemical Technology, Beijing 100029, P. R. China

Received December 1, 2003. Revised Manuscript Received February 12, 2004

In this paper a novel synthetic route of pure MFe_2O_4 (M = Mg, Co, and Ni) spinel ferrites is reported. The key feature of this method is using a single molecular precursor. The pure spinel ferrites can be obtained by calcination of tailored hydrotalcite-like layered double hydroxides (LDHs) of the type $[M_{1-X-Y}Fe^{2+}{}_{Y}Fe^{3+}{}_{X}(OH)_2]^{X+}(SO_4{}^{2-})_{X/2}\cdot mH_2O$ (M = Mg, Co, and Ni) precursors at 900 °C for 2 h, in which the molar ratio of $M^{2+}/(Fe^{2+} + Fe^{3+})$ is adjusted to the same value as that in single spinel ferrite itself. The structural characteristics of the as-synthesized LDHs and their resulting calcined products are obtained by powder X-ray diffraction (XRD), chemical analysis, Fourier transform infrared spectroscopy (FT-IR), simultaneous thermogravimetric and differential thermal analysis (TG-DTA), and Mössbauer spectroscopy. The saturation magnetizations of the materials produced by calcinations of LDHs are higher than those of the spinel ferrites produced by the conventional ceramic and wet chemical routes, although the compositions of the materials are similar. The major advantage of the new method is that it affords uniform distribution of all metal cations on an atomic level in the LDH precursors; hence, the formation of spinel ferrites starting from the LDHs requires a much lower temperature and shorter time, leading to a lower chance of side-reactions occurring.

Introduction

Spinels of the type $M^{2+}M^{3+}{}_2O_4$ attract a great deal of interest because of their diverse practical applications.[1,2] In the case of M^{2+} = Fe, the resulting spinel ferrites having a general chemical composition of MFe_2O_4 (M = Mn, Mg, Zn, Ni, Co, etc.), are among the most widely used magnetic materials.[3] Spinel has a face-centered cubic structure with a large unit cell containing eight formula units. There are two kinds of lattices for cation occupancy. A and B sites have tetrahedral and octahedral coordinations, respectively (Figure 1). Commonly, the M^{2+} and Fe^{3+} cations distribute at both sites. In a normal spinel the M^{2+} cations occupy tetrahedral sites and the Fe^{3+} cations occupy octahedral sites, whereas in an inverse spinel only half of the Fe^{3+} ions occupy tetrahedral sites. Actually, most spinel ferrites adopt a structure somewhere between these two extremes, so that the structural formula is usually written as $(M^{2+}{}_{1-c}Fe^{3+}{}_{c})\,[M^{2+}{}_{c}Fe^{3+}{}_{2-c}]\{O^{2-}\}_4$, where the round and square brackets denote (A) and [B] sites respectively and where c represents the degree of inversion [defined as the fraction of (A) sites occupied by Fe^{3+} cations]. The efficacy of the material depends on its microstructural properties that are sensitive to its mode of preparation,[4−6] which can play a very important role with regard to the chemical, structural, and magnetic properties of a spinel ferrite. To take magnesium ferrite, $MgFe_2O_4$, as an example, the conventional ceramic method of preparation[7] involves calcination of mixtures of precursors (MgO or $MgCO_3$ and Fe_2O_3) at considerably elevated temper-

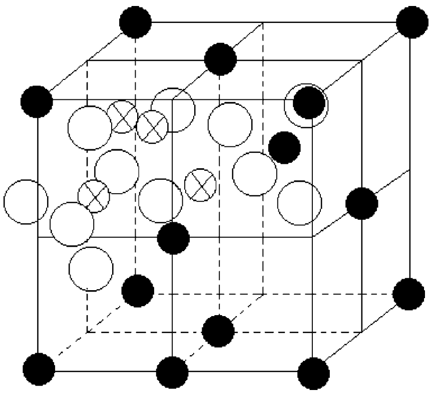

Figure 1. Schematic diagram for a partially filled unit cell of spinel AB_2O_4: ● A (tetrahedral coordination); ⊗ B (octahedral coordination); ○ oxygen.

---

* Co-corresponding authors. Tel: 8610-64412109. Fax: 8610-64425385. E-mail: lifeng_70@163.com or duanx@mail.buct.edu.cn.

(1) Hamdeh, H. H.; Xia, Z.; Foehrweiser, R.; McCormick, B. J.; Willey, R. J.; Busca, G. *J. Appl. Phys.* **1994**, *76*, 1135.

(2) Cheng, F.-X.; Jia, J.-T.; Xu, Z.-G.; Zhou, B.; Liao, C.-S.; Yan, C.-H.; Chen, L.-Y.; Zhao, H.-B. *J. Appl. Phys.* **1999**, *86*, 2727.

(3) Sugimoto, M. *J. Am. Ceram. Soc.* **1999**, *82*, 269.

(4) Yu, S. H.; Yooshimura, M. *Adv. Funct. Mater.* **2002**, *12*, 9.

(5) Pileni, M. P. *Adv. Funct. Mater.* **2001**, *11*, 323.

(6) Kulkarni, R. G.; Joshi, H. H. *J. Solid State Chem.* **1986**, *64*, 141.

(7) Šepelák, V.; Baabe, D.; Litterst, F. J.; Becker, K. D. *J. Appl. Phys.* **2000**, *88*, 5884.

10.1021/cm035248c CCC: $27.50

atures, such as 1100 °C or above. High temperatures with prolonged reaction time are required to prepare a single homogeneous phase but if the temperature is too high or the reaction time is too long there are problems with phase separation and nonstoichiometry.[8] Directed to this problem, new synthetic methods have received increased attention in recent years. For example, the mechanochemical route for the preparation of spinel ferrite has been reported starting from MO and α-Fe_2O_3 powder in equimolar ratio.[9−12] But in this method, the reactant is also the nonactivated α-Fe_2O_3/MO mixture, and actually it is especially difficult to achieve a single homogeneous spinel phase. Alternative wet chemical methods have been proposed, including coprecipitation from aqueous solution,[6] sol−gel synthesis involving supercritical drying to provide aerogels,[13] and use of micellar microemulsions.[5,14] In these cases, however, it is difficult to prevent contamination of the product by cations arising from the precipitants or organic residues from the precursor mixtures.[1] To avoid compromising the purity and properties of spinel ferrite and related materials it would be desirable to prepare them from a single solid precursor which can be prepared in a pure state in which the M^{2+} and Fe^{3+} cations are uniformly distributed on an atomic level.

Layered double hydroxides (LDHs), also known as hydrotalcite-like materials, are a class of synthetic two-dimensional nanostructured anionic clays whose structure can be described as containing brucite-like layers in which a fraction of the divalent cations have been replaced isomorphously by trivalent cations giving positively charged sheets with change-balancing anions between the layers.[15] LDHs have the general formula $[M^{2+}_{1-X}M^{3+}_{X}(OH)_2]^{X+}(A^{n-})_{X/n}\cdot mH_2O$, where M^{2+} and M^{3+} are di- and trivalent cations respectively, including Mg^{2+}, Fe^{2+}, Co^{2+}, Cu^{2+}, Ni^{2+}, or Zn^{2+} and Al^{3+}, Cr^{3+}, Ga^{3+}, Mn^{3+}, or Fe^{3+}, respectively; the value of the coefficient x is equal to the molar ratio of $M^{2+}/(M^{2+} + M^{3+})$; and A^{n-} is an anion, such as CO_3^{2-}, SO_4^{2-}, NO_3^{-}, F^{-}, Cl^{-}, or PO_4^{3-}.[16] Therefore, a large class of isostructural materials considered complementary to aluminosilicate clays with widely varied physicochemical properties can be obtained by changing the nature of metal cation, the molar ratio of M^{2+}/M^{3+}, and the type of the interlayer anion. These materials are potential precursors for spinel ferrites because they are often formed with mixtures of the same cations and have been shown to have an absence of long-range cation ordering.[17] Calcination of LDHs at intermediate temperatures (450−600 °C) affords poorly crystalline mixed metal oxides.[18] Calcination above 750 °C is known to give spinels, but these are always mixed with the oxide of divalent metal.[19] This reflects the fact that in LDHs, the divalent cations are always present in greater amount than the trivalent cations (the stoichiometric coefficient x above is found typically in the range 0.2−0.33, corresponding to the molar ratio of M^{2+}/M^{3+} of 2−4), whereas in a spinel the required molar ratio of M^{2+}/M^{3+} is 0.5.

In a recent investigation communication,[20] we briefly reported the preparation of LDHs of the type $[Mg_{1-x-y}Fe^{2+}_{y}Fe^{3+}_{x}(OH)_2]^{X+}(CO_3^{2-})_{X/2}\cdot mH_2O$, and shown how when the $Mg^{2+}/(Fe^{2+} + Fe^{3+})$ molar ratio in a LDH is 1:2, oxidation of all Fe^{2+} ions on calcination in air gives additional Fe^{3+} ions, thus overcoming the deficiency of trivalent ions, and leads to the formation of a pure $MgFe_2O_4$ spinel ferrite with excellent magnetic property. Because a wide variety of LDHs with three or more cations in the layers can be prepared, we report herein further work that has been carried out on the synthesis of a series of new tailored LDH precursors of the type $[M_{1-X-Y}Fe^{2+}_{Y}Fe^{3+}_{X}(OH)_2]^{X+}(SO_4^{2-})_{X/2}\cdot mH_2O$ (M = Mg, Co, and Ni) with the composition appropriate for stoichiometric synthesis of a range of pure spinel ferrites of commercial importance. The magnetic properties of the materials produced by calcinations of LDHs are compared with those of the spinel ferrites produced using the conventional ceramic and wet chemical methods.

Experimental Section

Synthesis of M-Fe^{2+}-Fe^{3+}-LDH sulfates (M = Mg, Co, and Ni). A mixture of $Fe_2(SO_4)_3$, $FeSO_4$, and $M(NO_3)_2$ (M = Mg, Co, and Ni) was dissolved in N_2-saturated deionized water ($[M^{2+} + Fe^{2+} + Fe^{3+}] = 0.8$ mol/L). A base solution ([NaOH] = 1.5 M) in N_2-saturated deionized water was added dropwise to the stirred mixture at 25 °C until the pH reached 11.0 for the reaction solution containing Mg^{2+} cations and 7.0 for the reaction solution containing Co^{2+} cations or Ni^{2+} cations. The resulting suspension was aged for 4 h in an N_2 atmosphere. The mixture was cooled by adding N_2-saturated deionized water at 0 °C, filtered, and washed with N_2-saturated deionized water at 0 °C and then N_2-saturated ethanol at 0 °C. The resulting solid was dried at room temperature and stored at 0 °C under N_2.

Synthesis of MFe_2O_4 Spinel Ferrites (M = Mg, Ni, and Co). For the LDHs precursors method the synthesized M-Fe^{2+}-Fe^{3+}-LDHs were calcined in air at 900 °C for 2 h at a heating rate of 10 °C/min and then the resulting products were slowly cooled to room temperature. For the conventional ceramic method a stoichiometric mixture of homogenized reactants containing powdered α-Fe_2O_3 and MO was sintered at 1100 °C for 10 h at a heating rate of 10 °C/min and the resulting product was slowly cooled to room temperature. For the wet chemical method the solution containing stoichimometric M^{2+} and Fe^{3+} cations was titrated with NaOH solution, and then the solid suspension was washed with deionized water, dried at room temperature, and calcined at 1100 °C for 10 h at a heating rate of 10 °C/min. The resulting product was slowly cooled to room temperature.

Characterization. Powder X-ray diffraction (XRD) patterns for the samples were recorded using a Shimadzu XRD-6000 diffractometer under the following conditions: 40 kV, 30

---

(8) O'Neill, H. St. C.; Annersten, H.; Virgo, D. *Am. Mineral.* **1992**, *77*, 725.

(9) Kaczmarek, W. A.; Campbell, S. J. *Bull. Magn. Reson.* **1996**, *17*, 148.

(10) Jovalekić, Č.; Zdujić, M.; Radaković, A.; Mitrić, M. *Mater. Lett.* **1995**, *24*, 365.

(11) Šepelák, V.; Steinike, U.; Uecker, D. Chr.; Wissmann, S.; Becker, K. D. *J. Solid State Chem.* **1998**, *135*, 52.

(12) Ding, J.; Yang, H.; Miao, W. F.; McCormick, P. G.; Street, R. *J. Alloys Compd.* **1995**, *221*, 959.

(13) Willey, R. J.; Oliver, S. A.; Oliveri, G.; Busca, G. *J. Mater. Res.* **1993**, *8*, 1418.

(14) Liu, C.; Rondinone, A. J.; Wang, Z. J. *Pure Appl. Chem.* **2002**, *72*, 37.

(15) Cavani, F.; Trifirò, F.; Vaccan, A. *Catal. Today* **1991**, *11*, 173.

(16) *Layered Double Hydroxides: Present and Future*; Rives, V., Ed.; Nova Science Publishers: New York, 2001.

(17) Vucelic, M.; Jones, W.; Moggridge, G. D. *Clays Clay Miner.* **1997**, *45*, 803.

(18) Vaccari, A. *Catal. Today* **1998**, *41*, 53.

(19) Fernández, J. M.; Ulibarri, M. A.; Labajos, F. M.; Rives, V. *J. Mater. Chem.* **1998**, *8*, 2507.

(20) Liu, J.; Li, F.; Evans, D. G.; Duan, X. *Chem. Commun.* **2003**, *4*, 542.

Table 1. Structural and Componential Parameters of the Synthesized M- Fe^{2+}-Fe^{3+}-LDHs

sample	Mg-Fe^{2+}-Fe^{3+}-LDH	Co-Fe^{2+}-Fe^{3+}-LDH	Ni-Fe^{2+}-Fe^{3+}-LDH
initial $M^{2+}/Fe^{2+}/Fe^{3+}$	3/5/2	3/5/2	3/5/2
initial $(M^{2+}+Fe^{2+})/Fe^{3+}$	4.000	4.000	4.000
initial $M^{2+}/(Fe^{2+}+Fe^{3+})$	0.429	0.429	0.429
$M^{2+}/(Fe^{2+}+Fe^{3+})$ in LDH[a]	0.493	0.493	0.516
lattice parameter[b] *a*, nm	0.314	0.315	0.313
lattice parameter[c] *c*, nm	3.300	3.311	3.335
ν (SO_4^{2-}), cm^{-1}	1098	1105	1111
δ (M−O−M), cm^{-1}	450	475	478
ν (M−O−M), cm^{-1}	596	621	621

[a] As determined by ICP. [b] c = average value calculated from (003), (006), and (009) diffractions. [c] $a = 2d_{110}$.

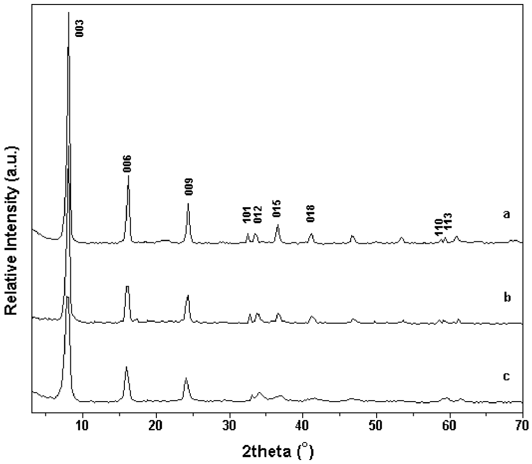

Figure 2. Powder XRD patterns for Mg-Fe^{2+}-Fe^{3+}-LDH (a), Co-Fe^{2+}-Fe^{3+}-LDH (b), and Ni-Fe^{2+}-Fe^{3+}-LDH (c).

mA, graphite-filtered Cu−Kα radiation (λ = 0.15418 nm). The samples, as unoriented powders, were step-scanned in steps of 0.04° (2θ) using a count time of 10 s/step. The observed interplanar spacings were corrected using elemental Si as an internal standard [d (111)= 0.31355 nm; JCPDS file 27-1402].

Elemental analysis for metal ions and sulfur in LDHs was performed using a Shimadzu ICPS-75000 inductively coupled plasma emission spectrometer (ICP-ES). Samples were dried at 100 °C for 24 h prior to analysis, and solutions were prepared by dissolving the samples in dilute hydrochloric acid (1:1). The H content in LDHs was determined by an Elementar Vario EL meter under the following conditions: carrier gas current 20 mL/min, oxygen current 20 mL/min, combustion tub temperature 950 °C, and reduction tub temperature 550 °C.

Fourier transform infrared spectra (FT-IR) were recorded in the range 4000 to 400 cm^{-1} with 2 cm^{-1} resolution on a Bruker Vector-22 Fourier transform spectrometer using the KBr pellet technique (1 mg of sample in 100 mg of KBr).

Simultaneous thermogravimetric and differential thermal analysis (TG-DTA) was carried out in air on a PCT-1A thermal analysis system produced locally. Samples of 9.0−10.0 mg were heated at a rate 10 °C/min up to 800 °C.

Mössbauer spectra were recorded with an Oxford MS-500 instrument at 293 K. A radiation source of Co^{57} in an Rh matrix was used. The isomer shifts are reported relative to sodium nitroprusside.

Magnetism of samples was measured at room temperature on a locally made JDM-13 vibration sample magnetometer.

Results and Discussion

Figure 2 illustrates the power XRD patterns for M-Fe^{2+}-Fe^{3+}-LDHs (M = Mg, Co, and Ni) with the $M^{2+}/Fe^{2+}/Fe^{3+}$ molar ratio of 3:5:2 in the synthesis mixture, and Table 1 summarizes the analytical properties of LDHs and relevant structural parameters of LDHs obtained from their XRD patterns. It can be noted clearly that the XRD patterns exhibit the characteristic diffractions of a hydrotalcite-like LDH material (JCPDS file 38-0487)[21] in each case and no other crystalline phases are present. The XRD patterns give a series of (00*l*) peaks, such as 003, 006, and 009, appearing as narrow symmetric lines at low 2θ angle, corresponding to the basal spacing and higher order diffractions, and indicate that the samples consist of a well crystallized single phase with large constituting crystallites. The elemental analysis of the LDHs gives the following formulas for M-Fe^{2+}-Fe^{3+}-LDHs (M = Mg, Co, and Ni): $[Mg_{0.33}Fe^{2+}_{0.27}Fe^{3+}_{0.40}(OH)_2]$ $(SO_4)_{0.20}\cdot 0.41H_2O$, $[Co_{0.33}Fe^{2+}_{0.27}Fe^{3+}_{0.40}(OH)_2]$ $(SO_4)_{0.20}\cdot 0.39H_2O$, and $[Ni_{0.34}Fe^{2+}_{0.28}Fe^{3+}_{0.38}(OH)_2]$ $(SO_4)_{0.19}\cdot 0.39H_2O$, respectively. Obviously, the experimental $M^{2+}/(Fe^{2+} + Fe^{3+})$ molar ratio employed in the final product in the range of 0.493−0.516 is significantly different from that in the corresponding synthesis mixture, but the values are reproducible within experimental error. This is because in the starting mixed aqueous solution partial Fe^{2+} cations have been oxidized to Fe^{3+} cations although the coprecipitation process is carried out under nitrogen atmosphere, and it also suggests that in the condition of holding molar ratio of $M^{2+}/Fe^{2+}/Fe^{3+}$ invariable, not all the metal cations can be coprecipitated completely.

LDH is a hexagonal system, where lattice parameter *a* is a function of the average distance of metal ions within the layers and reflects the density of metal ions stacking in 003 crystal plane, and lattice parameter *c* is three times the distance from the center of one layer to the next. Therefore, the incorporation of Mg^{2+}, Co^{2+}, and Ni^{2+} into the layers of LDH can be ascertained from the change in the lattice parameters *a* and *c*. Assuming a 3R stacking of the layers and from the positions of the (003), (006), (009), and (110) diffractions, although the latter (the lower angle component of the characteristic doublet close to $2\theta = 59°$) is rather broad and ill-defined, the lattice parameters *a* and *c* dependent on the composition of LDHs may be calculated[22] for LDH phases. As shown in Table 1, in accordance with the order of Ni-Fe^{2+}-Fe^{3+}-LDH, Mg-Fe^{2+}-Fe^{3+}-LDH, and Co-Fe^{2+}-Fe^{3+}-LDH, the lattice parameter a ($= 2d_{110}$) increases gradually, reflecting the fact that the Shannon ionic radii for octahedral Ni^{2+}, Mg^{2+}, and high spin Co^{2+} are 0.083, 0.086, and 0.089 nm, respectively. Furthermore, the value of lattice parameter c ($= d_{003} + 2d_{006} + 3d_{009}$) shows an increasing trend in accordance with the order of Mg-Fe^{2+}-Fe^{3+}-LDH, Co-Fe^{2+}-Fe^{3+}-LDH, and Ni-Fe^{2+}-Fe^{3+}-LDH, which can be explained mainly by

---

[21] Busetto, C.; Del Piero, G.; Mamara, G.; Trifirò, F.; Vaccari, A. *J. Catal.* **1984**, *85*, 260.

[22] Millange, F.; Walton, R. I.; O'Hare, D. *J. Mater. Chem.* **2000**, *10*, 1713.

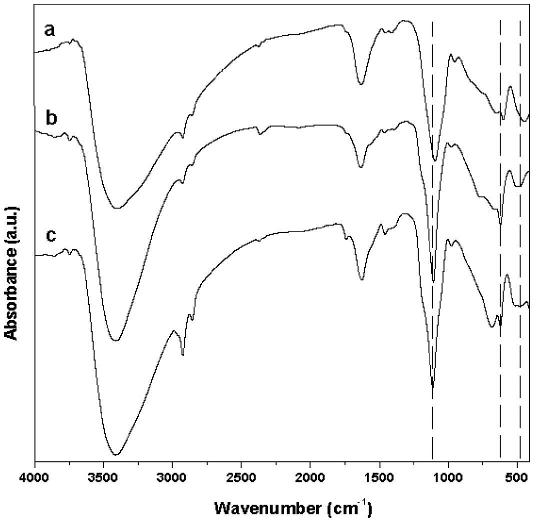

Figure 3. IR spectra for Mg-Fe^{2+}-Fe^{3+}-LDH (a), Co-Fe^{2+}-Fe^{3+}-LDH (b), and Ni-Fe^{2+}-Fe^{3+}-LDH (c).

the difference in bond strength between the cations and adjacent oxygen atoms on the layers of LDH. As it is well-known, the bond strength increases approximately 12.5% from Mg−O to Co/Ni−O[23] (Mg−O approximately 330 kJ/mol, Co−O approximately 368 kJ/mol, and Ni−O approximately 372 kJ/mol). The increasing bond-strength of M^{2+}−O results in the decrease in hydrogen-bond attractive force between M^{2+}−hydroxyl groups on the layers and the interlayer anions and water molecules, consistent with the decrease in Coulombic attractive force between the negatively charged interlayer anions and the positively charged brucite-like layers.

The FT-IR spectra for the LDHs in the region between 400 and 4000 cm^{-1} are shown in Figure 3. Typical of this spectrum[24] is the strong and broad absorption band between 3600 and 3200 cm^{-1} centered around 3450 cm^{-1} associated with a superposition of O−H stretching bands ν (OH_{str}) arising from metal−hydroxyl groups and hydrogen-bonded interlayer water molecules. Another absorption band corresponding to a water deformation, $\delta(H_2O)$, is recorded around 1620 cm^{-1}. There is absorption at around 1100 cm^{-1} which arises from the interlayer sulfate anions. The bands observed around 400−900 cm^{-1} are interpreted as the lattice vibration modes of M−O and M−OH.[25] On the basis of a detailed analysis of FT-IR spectra for the LDHs, more information (see Table 1) can be obtained. It can be seen that absorption bands of ν (M−O−M) and δ (M−O−M) shift to high frequency with the increasing bond strength of M−O. Furthermore, there is a small shift in the absorption band of the interlayer SO_4^{2-} at around 1100 cm^{-1} toward higher frequency in accordance with the order of Mg-Fe^{2+}-Fe^{3+}-LDH, Co-Fe^{2+}-Fe^{3+}-LDH, and Ni-Fe^{2+}-Fe^{3+}-LDH. This is due to a decrease in electron density around OH^- groups resulting in consequent reduction of hydrogen-bond attractive force between the M^{2+}-hydroxyl groups on the layers and the interlayer SO_4^{2-} anions, associated with the increasing bond strength of M^{2+}−O coordinated to OH^- groups.

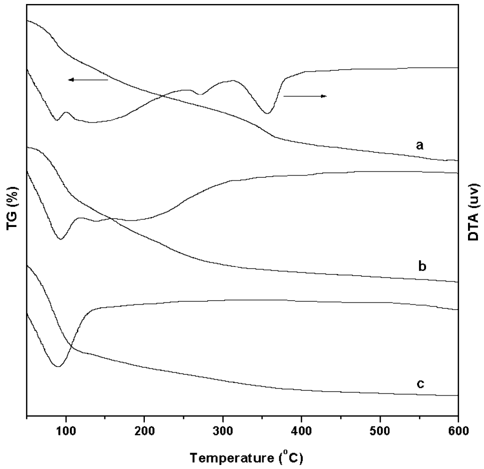

Figure 4. TG-DTA curves for Mg-Fe^{2+}-Fe^{3+}-LDH (a), Co-Fe^{2+}-Fe^{3+}-LDH (b), and Ni-Fe^{2+}-Fe^{3+}-LDH (c).

The structural stability of LDHs was examined by simultaneous TG/DTA experiments, with the TG and DTA curves shown in Figure 4. For Mg-Fe^{2+}-Fe^{3+}-LDH, the process for weight loss consists of four steps in the TG curve, and corresponds to four endothermic events in the DTA curve extending from room temperature up to ca. 400 °C, including desorption of water physisorbed on the external surface of the crystallites, removal of water intercalated in the interlayer galleries, dehydroxylation of the lattice, and decomposition of the interlayer sulfate anions, respectively. For Co-Fe^{2+}-Fe^{3+}-LDH there are three endothermic events in the DTA curves, including an obvious one at around 80 °C, a small one in the temperature range of 120−160 °C, and a particularly broad one in the temperature range of 160−350 °C. But for Ni-Fe^{2+}-Fe^{3+}-LDH, there exhibits only one big endothermic peak in the range of room temperature up to 150 °C. As a result, removal of interlayer water, dehydroxylation of the lattice, and decomposition of the interlayer sulfate anions are apparently more facile for Ni-Fe^{2+}-Fe^{3+}-LDH, as these events occur at lower temperatures than those observed for Mg-Fe^{2+}-Fe^{3+}-LDH and Co-Fe^{2+}-Fe^{3+}-LDH. This is also indicative of a decrease in the strength of hydrogen bonds between water molecules and interlayer anions, and thus a reduced electrostatic interaction between the layers and the anions which facilitates the process for weight loss, thus the structural transformation. This result is consistent with the XRD and FT-IR data discussed above.

Figure 5 displays the powder XRD patterns for the materials obtained by calcination of LDHs at 900 °C for 2 h in air. Obviously, calcination has destroyed the layered structure of the LDHs as no characteristic diffractions of LDHs are present in the XRD patterns for the calcined materials. In each case the characteristic diffractions of a spinel ferrite with good crystallinity are observed, and the XRD patterns for calcined LDH can be indexed to a pure spinel ferrite, consistent with the molar ratio of $M^{2+}/(Fe^{2+} + Fe^{3+})$ of 1:2 in the LDH precursor, which is the same as the stoichiometric ratio of M^{2+}/Fe^{3+} in a single MFe_2O_4 itself. Furthermore, the introduction of different M^{2+} cation gives a detectable change in the lattice parameter *a* for the synthesized cubic spinel phase. The value of the lattice parameter *a* for $MgFe_2O_4$, $CoFe_2O_4$, and $NiFe_2O_4$ ferrite is 0.8394,

---

(23) Kloprogge, J. T.; Frost, R. L. *J. Solid State Chem.* **1999**, *146*, 506.

(24) Hernandez-Moreno, M. J.; Ulibarri, M. A.; Rendon, J. L. *Phys. Chem. Min.* **1985**, *12*, 34.

(25) Titulaer, M. K.; Jansen, J. B. H.; Geus, J. W. *Clays Clay Miner.* **1994**, *42*, 249.

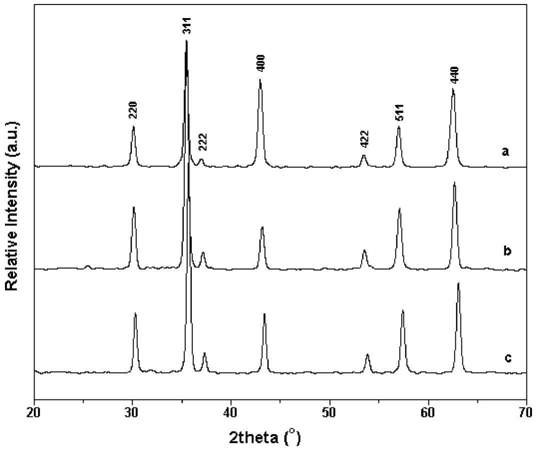

Figure 5. Powder XRD patterns for materials produced by calcinations of Mg-Fe^{2+}-Fe^{3+}-LDH (a), Co-Fe^{2+}-Fe^{3+}-LDH (b), and Ni-Fe^{2+}-Fe^{3+}-LDH (c).

0.8383, and 0.8338 nm, respectively. This indicates that the values of the lattice parameter vary as a function of the M^{2+} ionic radii but the relationship is not monotonic. This is probably because the lattice parameter can also be affected by the distribution of metal cations in the spinel structure,[26] which can directly influence the magnetic performance of materials. On the other hand, it can be seen from Figure 5 that the calcined LDHs exhibit narrow diffraction lines, probably indicative of a larger scattering domain size. The average crystallite size may be estimated from the values of the fullwidth at half-maximum (fwhm) of the (311), (400), and (440) diffraction peaks by means of the Scherrer equation [$L = 0.89\lambda/\beta(\theta)\cos\theta$],[22] where L is the crystallite size, λ is the wavelength of the radiation used (0.15418 nm), θ is the Bragg diffraction angle, and $\beta(\theta)$ is the fwhm. The average crystallite size for $MgFe_2O_4$, $CoFe_2O_4$, and $NiFe_2O_4$ ferrite is about 38.6, 49.0. and 42.0 nm, respectively.

Figure 6 shows room-temperature Mössbauer spectra for spinel ferrites taken in zero applied magnetic fields. Mössbauer spectroscopy studies have confirmed that there are partial overlaps of the two subspectra due to the small difference between the hyperfine fields of the iron atoms in the two sublattices for A and B sites, and no signals due to the existence of other phases such as Fe_2O_3 are observed, confirming that, as expected, the Fe cations in all samples have a +3 oxidation state, which implies that the typical composition for spinel ferrites is MFe_2O_4. Therefore, the major component in each case can be attributed to the two kinds of Fe^{3+} ions (A and B site) in a spinel ferrite phase. For MFe_2O_4 spinel ferrite the degree of inversion can be calculated from the relative areas of the Mössbauer subspectra.[27] Assuming the ratio of the recoilless fraction is $f_B/f_A = 0.94$ at room temperature, the Mössbauer parameters are given in Table 2. As a result, the structural formulas of the spinel ferrites obtained by calcinations of the LDHs are $(Mg_{0.47}Fe_{0.53})[Mg_{0.53}Fe_{1.47}]O_4$, $(Co_{0.15}Fe_{0.85})$-$[Co_{0.85}Fe_{1.15}]O_4$, and $(Ni_{0.12}Fe_{0.88})[Ni_{0.88}Fe_{1.12}]O_4$, respectively.

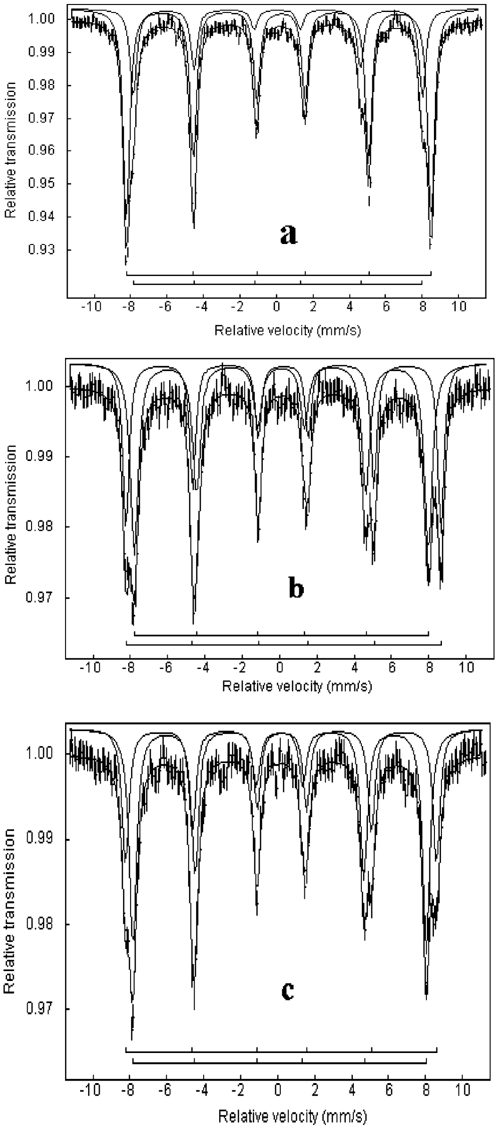

Figure 6. Mössbauer spectra for materials produced by calcinations of Mg-Fe^{2+}-Fe^{3+}-LDH (a), Co-Fe^{2+}-Fe^{3+}-LDH (b), and Ni-Fe^{2+}-Fe^{3+}-LDH (c).

The field dependence of the magnetization of synthesized spinel ferrites was measured using a vibrating sample magnetometer (VSM) at room temperature. The hysteresis loops of samples produced by calcination of LDHs at 900 °C for 2 h are shown in Figure 7. Clearly, the hysteresis varies with different samples, and the values of the saturation magnetization is evaluated by extrapolation of the magnetization vs 1/H to 1/H = 0. The saturation magnetization depends on the divalent metal ions and ranges from 35.0 for $MgFe_2O_4$, 50.6 for $NiFe_2O_4$, to 86.1 emu/g for $CoFe_2O_4$. As also shown in Table 3, the saturation magnetization of all spinel ferrites produced by calcination of LDHs have much higher values than those of MFe_2O_4 produced by conventional ceramic and wet chemical methods at 1100 °C for 10 h. This is because LDHs possess several advantages as a precursor to spinel ferrites that lead to enhanced saturation magnetization. Use of a molecular precursor with cations randomly distributed with no long order[18] facilitates the synthesis of a homogeneous spinel phase. The close structural relationship between the LDH precursor and its calcination products

---

(26) Navrotsky, A.; Kleppa, O. *J. Inorg. Nucl. Chem*. **1968**, *30*, 479.

(27) Šepelák, V.; Baabe, D. F.; Litterst, J.; Becker, K. D. *J. Appl. Phys.* **2000**, *88*, 5884.

Table 2. Mössbauer Parameters Measured at Room Temperature for Materials Produced by Calcinations of the LDHs[a]

	Mg-Fe^{2+}-Fe^{3+}-LDH			Co-Fe^{2+}-Fe^{3+}-LDH			Ni-Fe^{2+}-Fe^{3+}-LDH		
site	δ	ΔE	RA	δ	ΔE	RA	δ	ΔE	RA
(A)	0.025	0.125	25.31	0.084	0.005	42.64	0.100	0.0	41.99
[B]	0.151	0.013	74.69	0.200	0.005	57.36	0.201	-0.026	58.01

[a] (A) tetrahedral Fe^{3+} in MFe_2O_4; [B] octahedral Fe^{3+} in MFe_2O_4; δ(mm/s) isomer shift relative to sodium nitroprusside; ΔE(mm/s) quadrupole splitting; RA(%) relative intensity of peak areas.

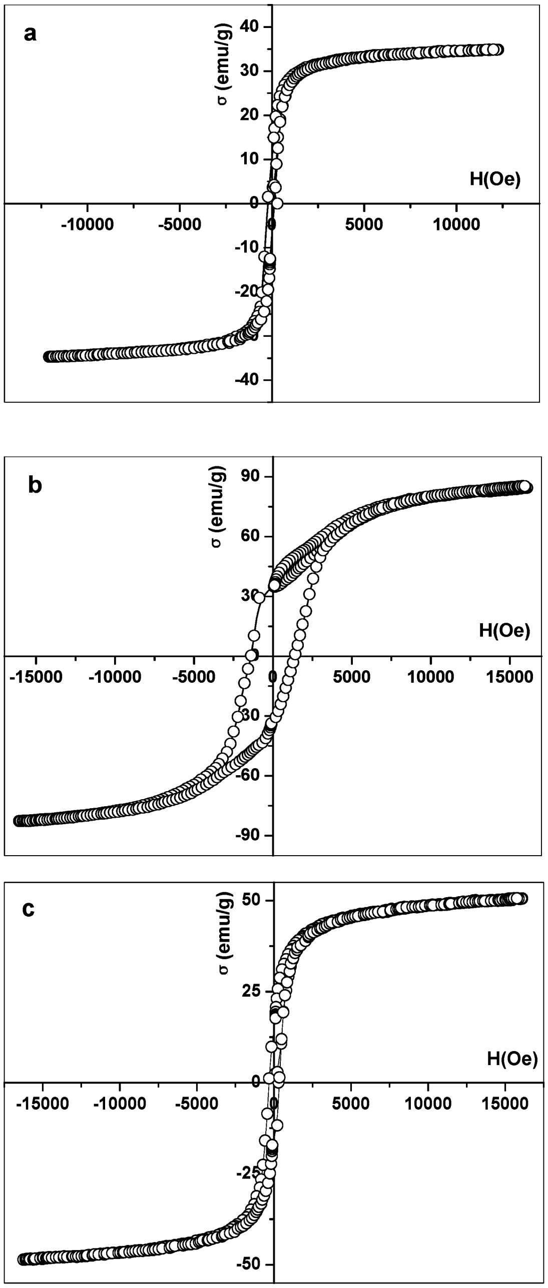

Figure 7. Hysteresis loops for materials produced by calcinations of Mg-Fe^{2+}-Fe^{3+}-LDH (a), Co-Fe^{2+}-Fe^{3+}-LDH (b), and Ni-Fe^{2+}-Fe^{3+}-LDH (c).

is also a key factor. Rebours et al. have shown that collapse of the layered structure on heating an LDH at around 400 °C gives a poorly crystalline mixed metal oxide, which can best be described as spinel-like phase.[28] This phase preserves the particle morphology of the LDH,[29] suggesting a topotactic transformation. In this case the (110) diffraction of the LDH transforms to the (440) spinel diffraction. Furthermore, the fact that the spinel is produced from a single solid precursor rather than a mixture means that the calcinations process requires a much shorter time and lower temperature, leading to a lower chance of side reactions occurring.

Table 3. Saturation Magnetization for Ferrites Produced by Different Methods

	saturation magnetization, emu/g		
method for preparation	$MgFe_2O_4$	$CoFe_2O_4$	$NiFe_2O_4$
LDHs precursors method	35.0	86.1	50.6
ceramic method	26.4	73.4	39.7
wet chemical method	26.6	73.1	40.6

Conclusions

A series of new pure layered double hydroxides (LDHs) as potential spinel ferrite precursors containing M^{2+} (M = Mg, Co, and Ni), Fe^{2+}, and Fe^{3+} cations in the brucite-like layers and having sulfate ions in the interlayer region with an $M^{2+}/(Fe^{2+} + Fe^{3+})$ molar ratio of 0.5 in the synthesis product have been prepared by coprecipitation method. Powder X-ray diffraction shows the presence of only one good crystalline phase. The detailed study on the structure of LDHs materials has shown that the change in the composition brought about by changing the M^{2+} cations results is small, but significant changes were observed in the lattice parameters and band positions of the modes for infrared adsorption. The TG/DTA analysis also indicates that in accordance with the order of Mg-Fe^{2+}-Fe^{3+}-LDH, Co-Fe^{2+}-Fe^{3+}-LDH, and Ni-Fe^{2+}-Fe^{3+}-LDH a decreasing the strength of hydrogen bonds between water molecules and interlayer anions, and thus a reduced electrostatic interaction between the layers and the anions, facilitates its structural transformation. Especially, Mössbauer spectroscopy and powder X-ray diffraction show that calcination of the tailored-type LDH precursor affords a pure MFe_2O_4 spinel ferrite. Furthermore, spinel ferrites derived from the LDHs precursors has higher saturation magnetizations than samples of the same materials produced by the conventional ceramic and wet chemical routes. The major advantage of the new method is that it affords uniform distribution of all metal cations on an atomic level in the LDH precursors; hence, the formation of spinel ferrites starting from the LDHs requires a much lower temperature and shorter time, leading to a lower chance of side reactions occurring.

Acknowledgment. We gratefully acknowledge the financial support from the National Science Foundation of China (20371006) and the Beijing Nova Program (2003B10).

CM035248C

---

(28) Bellotto, M.; Rebours, B.; Clause, O.; Lynch, J.; Bazin, D.; Elkaim, E. *J. Phys. Chem.* **1996**, *100*, 8535.

(29) Reichle, W. T.; Kang, S. Y.; Everhardt, D. S. *J. Catal.* **1986**, *101*, 352.